




RESEARCH ARTICLE

Light sedation with short habituation time for large-scale functional magnetic resonance imaging studies in rats

Lenka Dvořáková¹  | Petteri Stenroos^{1,2}  | Ekaterina Paasonen¹ |
Raimo A. Salo¹ | Jaakko Paasonen¹ | Olli Gröhn¹ 

¹A. I. V. Institute for Molecular Sciences,
University of Eastern Finland, Kuopio, Finland

²Grenoble Institut des Neurosciences,
Université Grenoble Alpes, Grenoble, France

Correspondence

Olli Gröhn, A. I. V. Institute for Molecular
Sciences, University of Eastern Finland,
P.O. Box 1627, FI-70211, Kuopio, Finland.
Email: olli.grohn@uef.fi

Funding information

Academy of Finland, Grant/Award Number:
298007; Horizon 2020 Framework Programme
of the European Union (Marie Skłodowska
Curie), Grant/Award Number: 740264

Traditionally, preclinical resting state functional magnetic resonance imaging (fMRI) studies have been performed in anesthetized animals. Nevertheless, as anesthesia affects the functional connectivity (FC) in the brain, there has been a growing interest in imaging in the awake state. Obviously, awake imaging requires resource- and time-consuming habituation prior to data acquisition to reduce the stress and motion of the animals. Light sedation has been a less widely exploited alternative for awake imaging, requiring shorter habituation times, while still reducing the effect of anesthesia. Here, we imaged 102 rats under light sedation and 10 awake animals to conduct an FC analysis. We established an automated data-processing pipeline suitable for both groups. Additionally, the same pipeline was used on data obtained from an openly available awake rat database (289 measurements in 90 rats). The FC pattern in the light sedation measurements closely resembled the corresponding patterns in both onsite and offsite awake datasets. However, fewer datasets had to be excluded due to movement in rats with light sedation. The temporal analysis of FC in the lightly sedated group indicated a lingering effect of anesthesia that stabilized after the first 5 min. In summary, our results indicate that the light sedation protocol is a valid alternative for large-scale studies where awake protocols may become prohibitively resource-demanding, as it provides similar results to awake imaging, preserves more scans, and requires shorter habituation times. The large amount of fMRI data obtained in this work are openly available for further analyses.

KEYWORDS

awake, fMRI, light sedation, rat, resting state fMRI

1 | INTRODUCTION

Functional magnetic resonance imaging (fMRI) is an effective noninvasive tool for studying the functional connectivity (FC) of the brain.¹ FC is altered in many central nervous system diseases, including Alzheimer's disease,² epilepsy,³ autism,⁴ Parkinson's disease,⁵ depression,⁶

Abbreviations used: ANTs, advanced normalization tools; EEG, electroencephalography; FC, functional connectivity; FDR, false discovery rate; FWD, framewise displacement; FWHM, full width at half maximum; GSR, global signal regression; ICA, independent component analysis; ROI, region of interest.

This is an open access article under the terms of the [Creative Commons Attribution-NonCommercial-NoDerivs](https://creativecommons.org/licenses/by-nc-nd/4.0/) License, which permits use and distribution in any medium, provided the original work is properly cited, the use is non-commercial and no modifications or adaptations are made.

© 2021 The Authors. *NMR in Biomedicine* published by John Wiley & Sons Ltd.

schizophrenia,⁷ bipolar disorder,⁸ and migraine.^{9–12} Importantly, similar FC network structures exist across species,^{13–16} which enables controlled studies of FC and its alterations to be conducted in established experimental animal-based disease models. Moreover, the fMRI assessment of FC can be combined with other cutting-edge techniques such as electrophysiology,^{17,18} optogenetics,^{19,20} positron emission tomography,²¹ calcium imaging,²² and histopathology. These combinations of methods can provide a wide range of information about FC from the cellular to the system level.

Typically, preclinical FC studies have utilized anesthetized animals because anesthesia reduces motion and stress in these animals during imaging. However, anesthesia greatly affects neuronal activity, neurovascular coupling, brain metabolism, and FC,²³ therefore, clearly awake imaging would be much more physiological. Another disadvantage of using anesthesia is that FC findings can be anesthetic- and dose-dependent. Subsequently, the use of anesthetics complicates the translation of results to clinical practice. These drawbacks led several groups to adopt awake imaging.^{16,24–26} Unfortunately, imaging in an awake state causes stress and discomfort for the animal, which subsequently induces its movement, leading to motion artefacts during imaging. These conditions require that there is a habituation protocol in an environment mimicking the actual measurement set-up. The habituation protocol periods have varied, lasting as long as 8 days with training sessions of up to 90 min per animal.²⁷ Although laborious, habituation can prevent a significant amount of animal movement during fMRI. Nonetheless, some level of spontaneous motion is unavoidable, and typically only part of the data can be utilized in data analysis. Because of the time-consuming training and the presence of some movement, awake imaging may become impractical in certain experiments, for example, in the large-scale studies required in the search for biomarkers or in the preclinical testing of drugs. Due to the above-mentioned challenges, only one large-scale study has examined the FC in the awake condition and even there, data was collected from various individual experiments performed over several years.²⁸ This lack of large-scale studies prevents a relevant evaluation of the intercenter reproducibility of FC in awake imaging.

One alternative for awake imaging is the use of a light sedation protocol; this would require shorter habituation times and, based on a preliminary study, could provide comparable FC results with awake-state measurements.²⁹ Therefore, our goal in this work was to demonstrate that a light-sedation protocol would be a valid and less resource-demanding alternative for fully awake imaging and thus suitable for large-scale trials. To achieve this, we scanned 102 rats in a lightly sedated condition and conducted both intracenter and intercenter comparisons with awake rat FC data.

2 | METHODS

2.1 | Animal preparations

Animal procedures were approved by the Finnish Animal Experiment Board. We habituated and measured 112 Sprague Dawley male rats (292 ± 39 g) either under light anesthesia (N = 102) or in an awake state (N = 10). The habituation followed a recently introduced protocol.²⁹ Briefly, rats were initially anesthetized with 5% isoflurane (lightly sedated group) or 5% sevoflurane (awake). Sevoflurane was used in the awake group according to a recommendation from the animal welfare committee to reduce the potential airway irritation associated with repeated short anesthesia during the training period. Isoflurane was used in the lightly sedated group to be consistent with our previous studies and general practice in the field. Rats were transferred to a heating pad and their front paws were tied alongside the body and their hind paws were taped together with the tail with masking tape. The rats were then wrapped in a sheet of foam, which was secured with masking tape around their shoulders and tail. Subsequently, the animals were placed on a rat bed with a restrainer, where the head was secured with a padded nose cone along with cheek, neck, and shoulder supports. A 3D-printed model of the receiver RF-coil was placed on top of the head and the bed was placed in a mock scanner. The level of anesthesia was lowered to 0.5% in the lightly sedated group and to 0% in the awake group, and the sound of the fMRI sequence was played, as described previously.²⁹ The groups were habituated in the mock scanner for either 3 (lightly sedated) or 4 (awake) consecutive days. The habituation time was gradually increased from 15 to 35 min for the lightly sedated, and for up to 45 min for the awake animals.

2.2 | Magnetic resonance imaging

The MRI measurements were performed with the 7-T/16-cm horizontal Bruker Pharmascan system. An actively decoupled standard Bruker quadrature resonator volume transmit coil and a quadrature surface coil pair optimized for rats were used. The breathing rate was followed during the imaging and the temperature of the animals was maintained with heated water circulation in the animal bed. While the animals were under anesthesia, scout imaging and global shimming were performed. The level of anesthesia was then lowered to either 0% in awake or 0.5% in the lightly sedated group, and automated local shimming for the rat brain was performed using a field map-based approach. After the animal showed signs of alertness (breathing rate >95 breaths per min or clear movement) or enough time had elapsed (5 min), the fMRI was started. fMRI data were acquired with a gradient-echo echo-planar imaging sequence for 25 min (1500 repetitions) with the following parameters: repetition time 1 s, 17 slices, slice thickness 1 mm, no gaps between slices, matrix size 64 × 64, field of view 3 × 3 cm², and saturation slabs in four

directions. After completion of the fMRI scan, the isoflurane was increased to 3% until the rat was in the anesthetized state, as indicated by its breathing rate.

2.3 | Data preprocessing

Raw fMRI data were converted to NIfTI (<http://aedes.uef.fi>) and slice-timing corrected (SPM8). To eliminate reconstruction-related artifacts in the border slices, the first and last slice were excluded from further analysis. Volumes with excessive motion were discarded using a motion-scrubbing approach.²⁸ Altogether, six degrees of transformation were estimated, including translation in the three orthogonal axes and rotation around these axes. The framewise displacement (FWD) for the frame i was calculated as $FWD_i = |\Delta x_i| + |\Delta y_i| + |\Delta z_i| + r \cdot (|\Delta \alpha_i| + |\Delta \beta_i| + |\Delta \gamma_i|)$, where $x_i, y_i,$ and z_i were translations in the three orthogonal axes, $\alpha_i, \beta_i,$ and γ_i are the rotation around the three orthogonal axes for the frame i , and r is the radius of displacement (set to 5 mm). Volumes exceeding the threshold of FWD 0.30 mm and the neighboring volumes were discarded. Data were then motion-corrected and coregistered to a reference brain using advanced normalization tools (ANTs; <http://stnava.github.io/ANTs/>³⁰) and spatially smoothed (FWHM = $0.8 \times 0.8 \times 0.8$ mm, SPM8). Additionally, the motion was estimated from the parameters obtained during the motion-correction step and used for further analysis. Moreover, an independent component analysis (ICA; <https://fsl.fmrib.ox.ac.uk/fsl/fslwiki/MELODIC>) was performed for each subject. The non-neuronal components were automatically selected from the obtained 30 components and regressed out. We set two criteria to flag the component as non-neural: (1) when the correlation of the time series of the component with one of the motion parameters exceeded 0.7, and (2) when more than 55% of the spatial map voxels were located in the edge regions of the brain. Those scans with more than flagged 20/30 components were not considered in the subsequent analysis.

When assessing the data quality, the FWD was calculated from the motion estimates before and after the motion-scrubbing step with the parameter $r = 5$ mm in the lightly sedated and the open database groups²⁸ in all scans. The first 300 volumes were excluded in the lightly sedated group to ensure stabilization of the FC. Due to the different numbers of volumes in the onsite and open database groups, only the first 600 volumes were considered in the analysis of both groups. A diagram illustrating the volume selection for this and all following analysis in the lightly sedated group is available in Figure S1.

2.4 | FC analyses

2.4.1 | Regions of interest and data selection

In the analyses of regions of interest (ROIs), a set of 21 ROIs was drawn on the reference brain according to an anatomical atlas³¹ to allow a detailed comparison of our data with both the onsite-measured awake data and the awake rat fMRI open database,²⁸ and to explore the lateral connectivities. The mean ROI signals were bandpass-filtered (0.01–0.1 Hz). A sliding window (150 volumes) was used to automatically select the motion-free parts of the signal based on displacement of the center of mass. To ensure a continuous signal for the fMRI analysis, windows where 10% or more of volumes had been excluded during the motion-scrubbing step were not used in the subsequent analysis. Unless stated otherwise, 300–1050 motion-free volumes were selected in each measurement and the signal from those windows was concatenated. The Pearson correlation of each ROI pair mean time series was calculated in each window, while the displacement of the center of mass in the three translation directions served as a regressor to minimize the influence of a non-neural signal on the correlation value. The correlation coefficient of each ROI was then calculated as the mean value from the windows.

2.4.2 | Temporal differences in FC in the lightly sedated group

To evaluate the potential lingering effect of the high initial isoflurane dose on FC in the lightly sedated group, we compared the FC matrices obtained from windows located in the beginning, in the middle, and at the end of the acquired 1500 volumes. In this dynamic analysis, 150 consecutive volumes with the least displacement of the center of mass from the window of 300 volumes starting from the first, 300th, and 1200th volumes were included in this analysis.

2.4.3 | Intracenter comparison of FC obtained with lightly sedated and awake animals

To assess the comparison of the onsite-measured awake and lightly sedated animals, we compared the FC matrices acquired with the set of 21 ROIs. The first 300 volumes (5 min) were not considered in both groups to ensure the stability of the state of consciousness.

2.4.4 | Comparison of FC in the lightly sedated group with the large awake rat database

The same data preprocessing and analysis pipeline was applied to the open dataset of resting-state fMRI in awake rats (289 measurements in 90 rats),²⁸ with the exception that the motion-free periods were searched in all available volumes. As in the previous analysis, the first 300 volumes were discarded in the analysis in the lightly sedated group. Additionally, we used an ROI including everything but brain as an additional regressor prior to bandpass filtering in both datasets. In both datasets, scans where more than 20/30 components were removed in the ICA-based motion-correction step were completely discarded from the FC analysis. In 51/289 (18%) of the awake database and 4/102 (4%) of the lightly sedated group, less than two windows of length 150 volumes were found to be suitable due to the motion scrubbing and therefore were also excluded from the analysis. In addition, scans where the correlation of the signal from nearby muscle tissue to the mean signal from the brain exceeded 0.3 were discarded. Subsequently, 81/102 (79%) scans from the lightly sedated group and 198/289 (69%) from the open awake rat fMRI database remained in the FC analysis.

In addition to the previous preprocessing steps, we performed a global signal regression (GSR) in both groups. The signal from the brain mask was used as a regressor after the outer signal regression and prior to the bandpass filtering. Next, the FC analysis was performed, and the specificity of FC was investigated in both datasets. In the FC specificity assessment, we modified a previously described method.³² Briefly, the correlation between the somatosensory cortex (S1S2) and the contralateral somatosensory cortex (S1S2_L) was selected as a specific and the correlation between the S1S2 and the cingulate cortex (CG) was designated as a nonspecific correlation. Based on the correlation values of these connections, the individual scans were sorted into four categories: specific, nonspecific, spurious, and no FC; the parameters for the categorization are summarized in Table 1.

2.4.5 | Group-level ICA analysis

A group-level ICA (45 components, <https://fsl.fmrib.ox.ac.uk/fsl/fslwiki/MELODIC>) was conducted on the lightly sedated group, including all 102 animals that had undergone the preprocessing steps (motion scrubbing, motion correction, smoothing, and coregistration). The components were then registered to the SIGMA anatomical brain template³³ with ANTs using affine and nonlinear SyN registration.³⁴ Any remaining non-neuronal components with an unspecific anatomical localization were excluded from the results.

2.4.6 | Statistical analysis

The statistical analysis was performed in MATLAB and RStudio (RStudio Team, <http://www.rstudio.com/>). The differences between the correlation values are presented as mean \pm standard deviation. In all statistical evaluations, Fisher z-transformation was applied to the correlation values. In the awake database, multiple correlation coefficients or FWDs of each subject were first averaged before the statistical analysis. We explored the temporal variability in the lightly sedated group by fitting a linear mixed model, where subject and ROI pair were modeled as random effects. In the comparison between the lightly sedated group and the database, a two-sample t-test was used, and finally, in the comparison between the lightly sedated and onsite-measured awake group, a studentized permutation test was used.³⁵ All *p*-values that were false discovery rate (FDR)-corrected³⁶ are noted as *q*. Values of *p* less than 0.05 and of *q* less than 0.05 were considered statistically significant.

3 | RESULTS

3.1 | Motion of the animals

Figure 1 shows the distributions of the mean FWD in the lightly sedated and awake database groups before and after the motion scrubbing. Before motion scrubbing, the global mean FWD was 0.079 mm in the lightly sedated group and 0.075 mm in the awake rat database. After

TABLE 1 Categorization criteria for the specificity analysis

Type of functional connectivity	Correlation threshold for specific connectivity	Correlation threshold of nonspecific connectivity
Specific	>0.1	<0.1
Nonspecific	<0.1	>0.1
Spurious	<−0.1	<−0.1
None	>−0.1 and <0.1	>−0.1 and <0.1

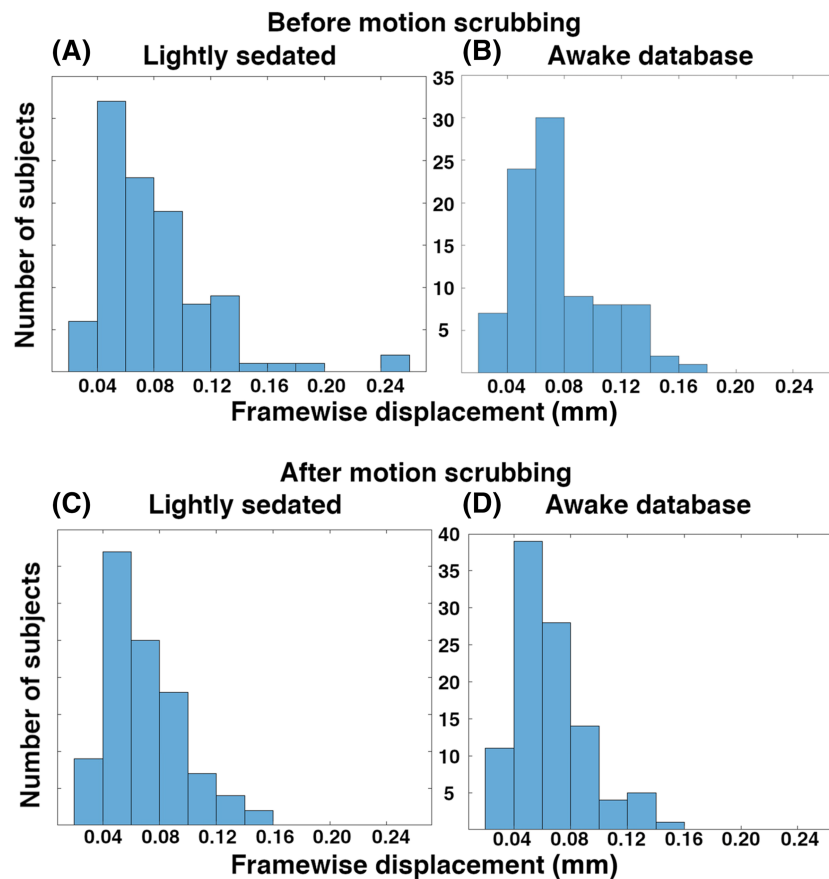


FIGURE 1 Distribution of the framewise displacement in the (A) Lightly sedated group ($N = 102$) and (B) Awake openly available database group ($N = 89$) before motion scrubbing, and in the (C) Lightly sedated group ($N = 102$) and (D) Awake openly available database group ($N = 89$) after motion scrubbing. There was a statistical difference in the means between the groups both before and after motion scrubbing (two-sample t-test, $p < 0.05$)

motion scrubbing, the global mean FWD was 0.069 mm in the lightly sedated group and 0.056 mm in the awake rat database, which indicates that the motion scrubbing had indeed reduced the effect of motion in the data. Even although the differences between groups both before and after motion scrubbing were statistically significant ($p < 0.05$, two-sample t-test), the differences of the global means were small (<0.004 and <0.013 mm before and after motion scrubbing, respectively) relative to voxel size ($0.47 \times 0.47 \times 1.00 \text{ mm}^3$) and the distributions of the FWD were similar. This indicates that the different habituation protocols and motion scrubbing resulted in similar motion-wise data in both large datasets.

The maximum value of each transformation direction of each individual scan is shown in Figure S2. When evaluating the gross movement in the lightly sedated group, we calculated the ratio of volumes within one scan with translation values lower than 1, 0.5, 0.2, and 0.1 voxels and rotation values lower than 3, 2, 0.5, and 0.2 degrees. Apart from a couple of outliers, all the scans showed a translation lower than 1 voxel and a rotation lower than 3 degrees in all volumes. Moreover, three out of every four of the scans had a translation value lower than 0.2 voxels in more than 70% of the volumes and a rotation value lower than 0.5 degrees in 80% of the volumes. Only about every fourth scan had a translation value higher than 0.1 voxels in more than 55% of the volumes and a rotation value higher than 0.2 degrees in more than 40% of the volumes.

3.2 | FC analysis: Temporal variability in the lightly sedated group

We explored the temporal variability in the lightly sedated group by comparing the FC values obtained with the 21 ROIs (Figure 2). The fitted linear mixed model showed a linear trend between the time points, and residuals were normally distributed. Nevertheless, the differences between the three different time points were very small. The mean difference between the first and last time point was only 0.036 ± 0.027 , and the mean FC change rates were (0.0042 ± 0.0032) 1/min and (0.0018 ± 0.0014) 1/min between the first and second, and second and third time points, respectively. This indicates that even although a lingering effect of initial anesthesia was present during the whole measurement, the difference

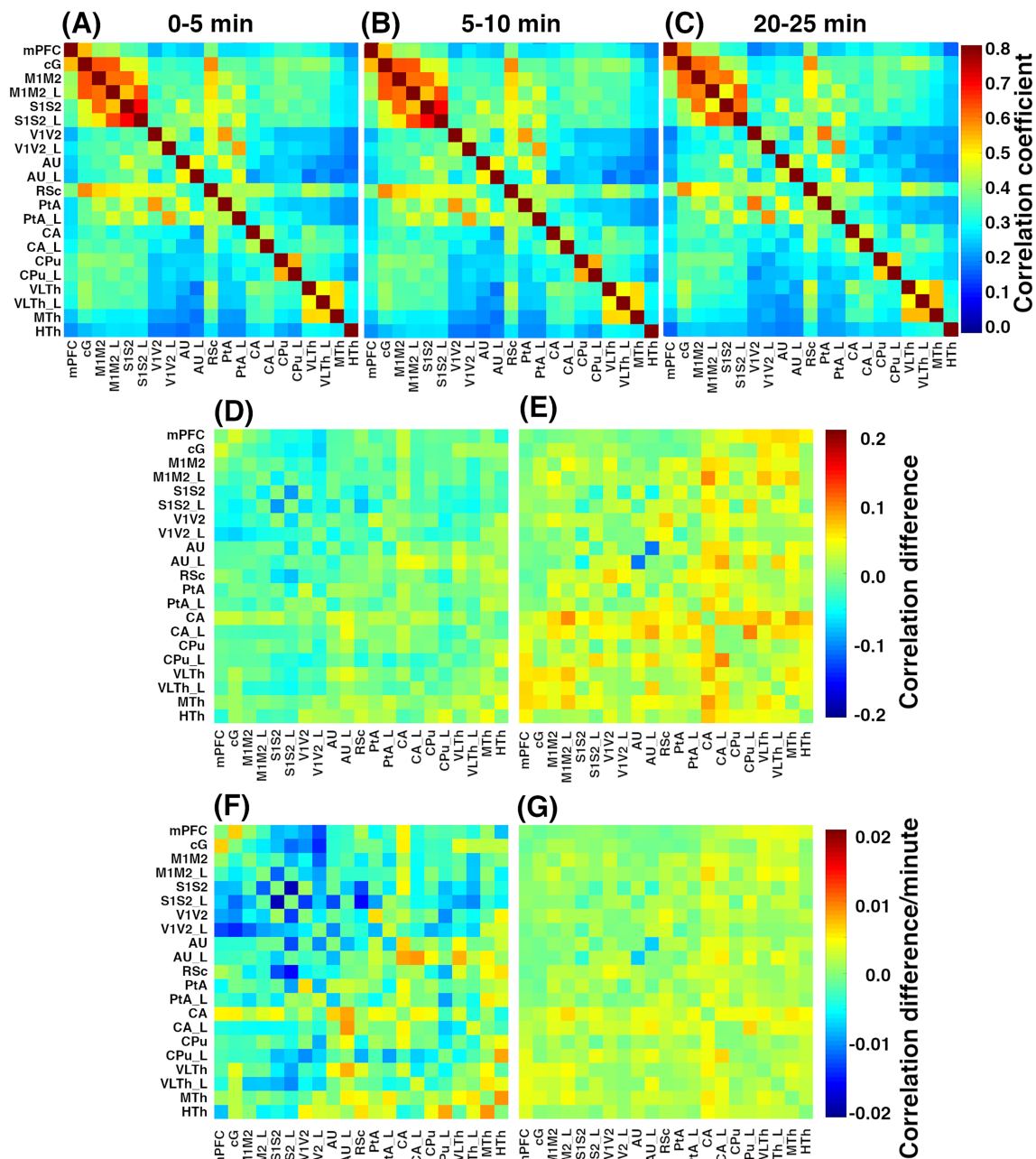


FIGURE 2 The mean functional connectivity (FC) matrices of the onsite-measured lightly sedated animals at intervals of (A) 0–5, (B) 5–10, and (C) 20–25 min. In the second row, the difference matrices are shown between the (D) First and second time point, and the (E) Second and third time point. In the third row, the rate of the correlation change is shown between the (F) First and second time point, and the (G) Second and third time point. Region of interest (ROI) annotation: AU, auditory cortex; CA, hippocampus; cG, cingulate cortex; CPu, caudate putamen; HTh, hypothalamus; M1M2, motor cortex; mPFC, medial prefrontal cortex; MTh, medial thalamus; Nacc, nucleus accumbens; RSc, retrosplenial cortex; S1S2, somatosensory cortex; V1V2, visual cortex; VLTh, ventrolateral thalamus; the bilateral ROIs are denoted by L for the left side

attributable to its presence was minor, especially after the first 5 min of data acquisition. As an extra precaution, we decided to exclude the first 5 min of the measurement.

3.3 | FC analysis: Comparison of the lightly sedated group with the onsite awake group

The comparison of FC matrices between the onsite-measured lightly sedated and awake animals is shown in Figure 3. The differences of the correlation coefficients were small (0.085 ± 0.080) and the correlation between the two correlation matrices was high ($R^2 = 0.59$, $p < 0.05$). Only one

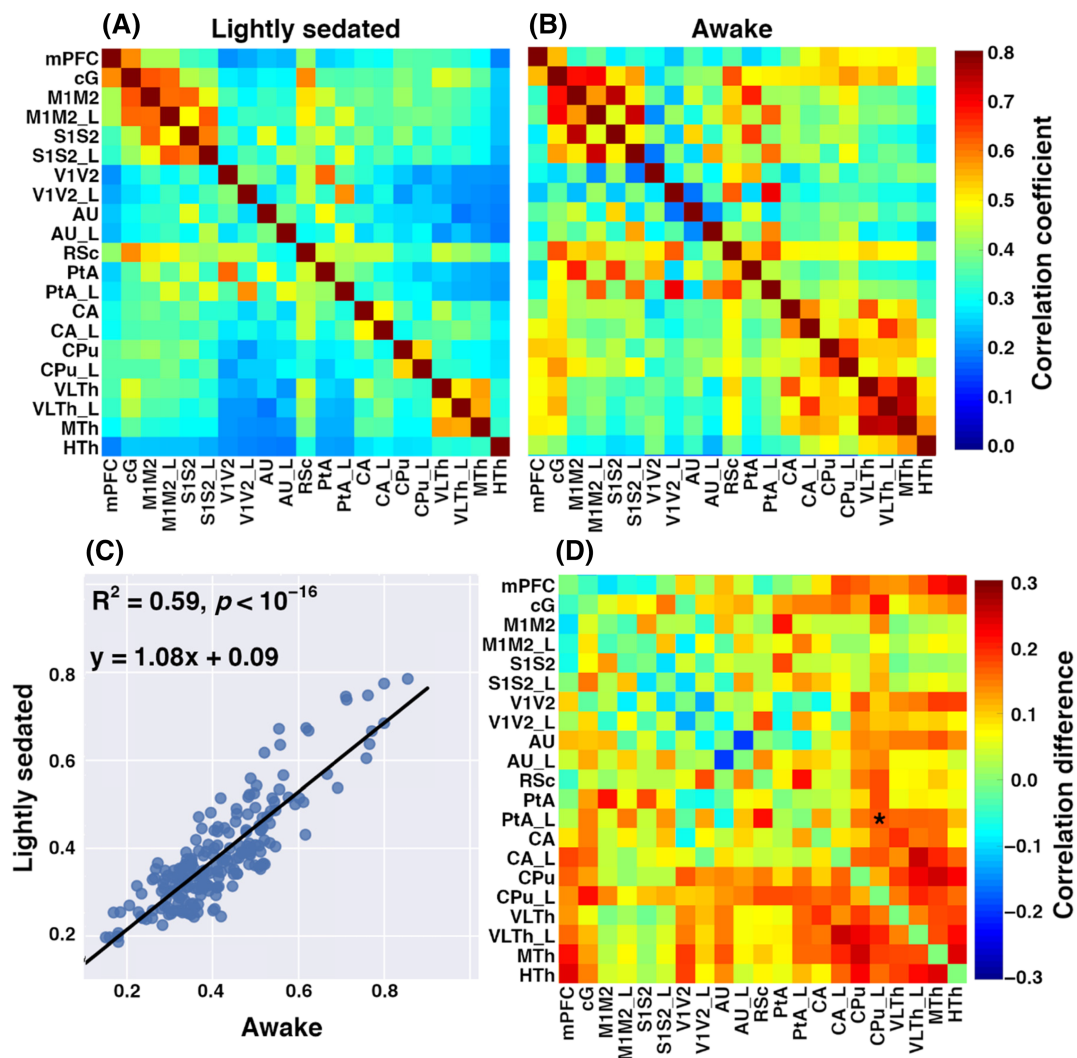


FIGURE 3 The mean functional connectivity (FC) matrices of the onsite-measured (A) Lightly sedated ($N = 81$) and (B) Awake ($N = 9$) animals, and their (C) Corresponding correlation. (D) Differences between the onsite-measured awake and lightly sedated FC values (false discovery rate-corrected studentized permutation test, $*q < 0.05$). Note that the region of interest annotation is the same as for Figure 2

ROI pair in the lightly sedated animals exhibited a statistically different correlation value compared with the awake animals ($q < 0.05$, studentized permutation test, FDR-corrected), emphasizing the overall similarity of the matrices. Importantly, this observation was in line with our previous results obtained with a different fMRI sequence.²⁹

3.4 | FC analysis: Intercenter comparison of the lightly sedated rats with the open awake rat database

The FC pattern in the lightly sedated group was very similar to the one obtained from the awake rat fMRI database (Figure 4), as the correlation between the corresponding correlation values in the two datasets was high ($R^2 = 0.75$, $p < 0.05$). In more detail, in both datasets we observed low correlation values in the hypothalamus, whereas the correlation values in the cortico-cortical pairs revealed only a couple of statistically significant differences. However, thalamo-hippocampal, thalamo-cortical, and cortico-hippocampal correlation values were slightly higher in the awake dataset. Out of 210 ROI pairs, 95 showed a statistically significant difference ($q < 0.05$, two-sample t-test, FDR-corrected). However, the absolute differences between the correlation values in the database and the lightly sedated groups were small (0.041 ± 0.059). The standard deviation of the FC was significantly lower in the lightly sedated group compared with the database ($q < 0.05$, two-sample t-test, FDR-corrected), evidence of the lower intersubject variability in the lightly sedated group.

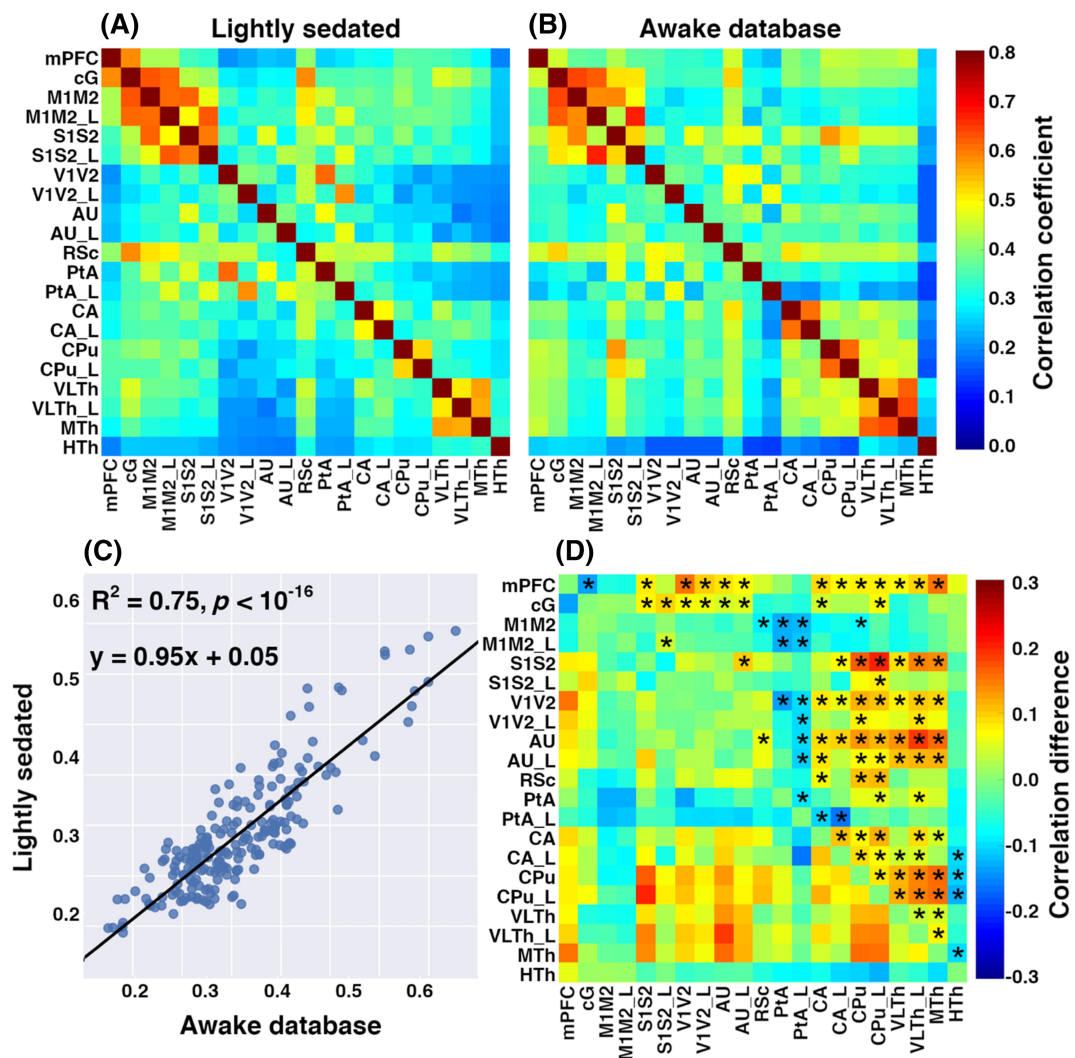


FIGURE 4 The mean functional connectivity (FC) matrices of the (A) Onsite-measured lightly sedated animals (N = 81) and (B) Offsite awake rat database (N = 198), and their (C) Corresponding correlation. (D) Differences between the openly available awake rat database and lightly sedated FC values (false discovery rate-corrected t-test, $*q < 0.05$). Note that the region of interest annotation is the same as for Figure 2

The FC matrices with GSR are shown in Figure S3. Similar to the analysis without GSR, we observed higher cortico-subcortical correlation values in the awake database. Even although the differences in the cortical regions were more pronounced than in the analysis without GSR, the correlation between the two datasets was still reasonable ($R^2 = 0.55, p < 0.05$).

We further explored the specificity of the FC in both lightly sedated and awake database groups. In the lightly sedated animals, we found that 68.7%, 21.7%, 4.8%, and 4.8% scans belonged to specific, unspecific, spurious, and no FC groups, respectively. In the awake database, 44.3%, 25.3%, 10.1%, and 20.2% of scans showed specific, unspecific, spurious, and no FC, respectively. The findings are shown in Figure S4 and are in line with previous reports in the literature.^{28,32,37} Therefore, we observed a higher representation of the specific FC group in the lightly sedated dataset than in the awake rat database.

3.5 | Group-level ICA

We created ICA spatial maps in well-localized brain regions, including the insular area, sensory and motor cortex, cingulate, forebrain, hippocampus, striatum, amygdala, thalamus, and hypothalamus (Figure 5). These corresponded well with the components obtained in the openly available database with awake rats.²⁸ Only the component covering the midbrain regions was missing in our data, likely because of the limited coverage in our data acquisition. All 45 ICA components are shown in Figure S5.

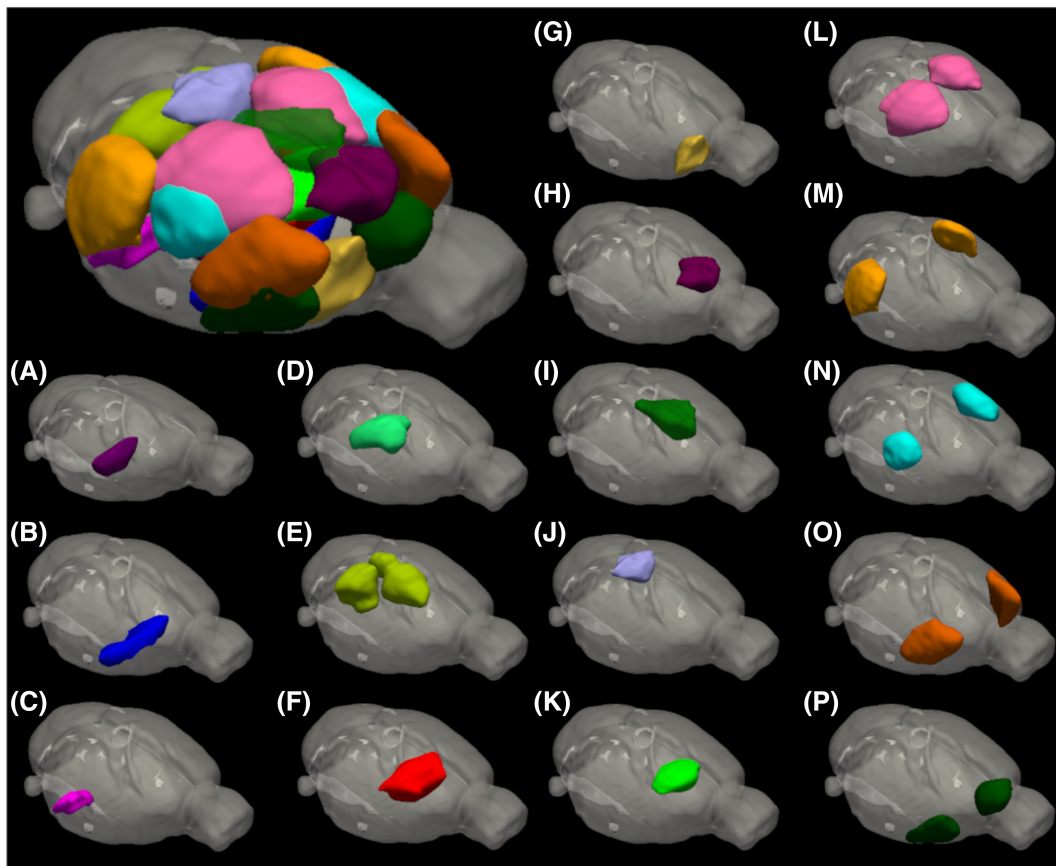


FIGURE 5 The spatial probability maps of 21 ICA components in (A–C) Hypothalamus, (D) Thalamus, (E) Hippocampus, (F) Striatum, (G) Forebrain, (H–K) Cingulate, (L–O) Sensory and motor cortex, and (P) Insular areas. Components from bilateral regions are shown together in the individual maps. The z-score threshold given by MELODIC or higher is used for illustration purposes. The detailed spatial distribution and z-score thresholds of individual components are shown in Figure S5. ICA, independent component analysis

4 | DISCUSSION

In this study, we aimed to demonstrate that a light sedation protocol can provide a valid alternative to fully awake imaging in large-scale studies. To achieve this goal, we measured the FC in 102 rats under 0.5% isoflurane sedation (i.e. we compared the outcomes with onsite lightly sedated data with both onsite-measured awake data and an offsite-measured large awake rat openly available database).²⁸ We demonstrated that the FCs indeed showed similar patterns in the lightly sedated group to both sets of awake data. Importantly, these results were achieved with only 3 days of habituation with the light sedation, while the open awake rat database protocol demanded 7 days of habituation. Moreover, less data were excluded due to motion with the light sedation than had been needed with the open awake rat database.

Overall, results from the lightly sedated group differed only slightly from both onsite and offsite awake groups. The onsite awake data showed only small differences to the lightly sedated group, which is in line with our previous results.²⁹ When we compared the lightly sedated and offsite awake group, we observed that the absolute differences in the correlation coefficients were predominantly below 0.1 and always lower than 0.2, and furthermore the pattern of the FC values was similar. The differences are, however, more widespread than those that we previously observed,²⁹ but in this study, there is a considerably greater number of animals increasing the experiment's statistical power. Additionally, differences in imaging protocols may explain some of the differences in the results, although their exact contribution remains unknown. The specificity analysis showed a good representation of the specific FC in both groups. The lightly sedated group even showed that almost as many as 70% of the scans belonged to the specific FC group. Despite the possibility that even a low level of anesthesia can hinder the detection of certain resting-state networks,³⁸ the spatial maps obtained with the group ICA in the lightly sedated group revealed similar structures to the awake data,²⁸ supporting the validity of the lightly sedated protocol. Moreover, the lightly sedated group also showed lower intersubject variability, suggesting that the lightly sedated protocol yields more stable baseline fluctuations.

While comparing the lightly sedated and offsite awake groups, we explored the FC both with and without GSR. There has been an extensive discussion about the use of GSR during the preprocessing of fMRI data. Even although some studies have shown that GSR improved the anatomical specificity of the fMRI analysis,^{39,40} or reduced the effect of anesthesia,⁴¹ the true origins of the global signal are not clear.⁴² Apart from the

non-neuronal influences such as scanner artifacts and motion,⁴³ there has been evidence that GSR also removes neuronal contributions.^{40,42} Moreover, due to the properties of GSR, the negative correlation introduced by GSR can be artifactual.^{40,44} For these reasons, our focus was on the analysis without undertaking GSR. However, we applied GSR while studying the specificity of FC, to be consistent with the original work introducing the quality index used in the current work.³²

We observed slightly higher correlation values in the cortico-cortical regions in the lightly sedated group in comparison with the offsite awake data. A possible explanation for this observation is that a low dose of anesthesia can induce large-amplitude slow EEG waves in the cortical region.^{45,46} Even although the exact relationship between the EEG and fMRI signal has yet to be confirmed, it is possible that slow and large-amplitude waves in electrical activity are reflected in the BOLD signal, which could subsequently increase the correlation coefficients. The decrease in the connectivity in subcortical and cortico-subcortical regions may also be an effect of isoflurane anesthesia (e.g. a low level of isoflurane can suppress hippocampal activity).^{29,47,48} These present observations are in agreement with our previous findings.²³ Nevertheless, the differences between lightly sedated and awake groups can be considered as minor with respect to the impact on FC of full anesthesia.^{23,29,41} In addition to the generally slightly lower FC values, the use of a light sedation protocol has some limitations. The effects of isoflurane on FC and gene expression are speculated to last for at least 1 month after a single exposure,⁴⁹ a problem that is encountered in all experiments using isoflurane. However, one typically cannot avoid anesthesia, even in the fully awake protocol, as this drug is used to calm the animal during the preparation steps. The constant exposure to isoflurane in the lightly sedated protocol can be considered a limitation, but on the other hand, the habituation period in the awake protocol requires more days, resulting in increased repetitive daily isoflurane exposure.

In the lightly sedated group, we observed temporal changes in FC that could be caused by the lingering effects of isoflurane. Even although isoflurane is cleared from the bloodstream within 7–10 min,²⁵ in a recent study, immediate effects in the brain were recorded as late as 30 min after cessation of the anesthesia.⁵⁰ We observed a linear trend of the FC during the acquisition, but the observed differences were very small and can be considered as a minor nuisance factor.

Anesthesia can hinder the detection of certain resting-state networks and the differences in the detected networks can be anesthesia-dependent.⁵¹ On the other hand, a recent study has shown the same resting-state networks in awake, lightly sedated (0.8% isoflurane) and anesthetized (isoflurane and medetomidine) mice.³⁷ However, it has been shown that anesthesia mainly influences the subcortical networks.³⁸ The spatial maps obtained with the group ICA in our lightly sedated group were located in both the cortical and subcortical regions. These corresponded well with published awake data.^{16,28,37} Our data, therefore, reveal good agreement of the observed network structures; however, to conduct a better comparison, graph theory should be examined.

Motion is a common confounder in awake fMRI measurements.⁵² Even although motion is markedly diminished with the habituation procedure, some motion still occurs during the data acquisition with both the awake and light sedation protocol. Some special procedures have been implemented, such as using a paralyzing agent⁵³ or alternative pulse sequences that are not as sensitive to motion as conventional fMRI sequences.¹⁷ Furthermore, additional steps in the preprocessing pipeline, apart from the classical motion correction, have been established to minimize the effect of motion on data. Some investigators have exploited a motion-scrubbing approach to remove the volumes with high FWD to minimize the motion artefacts,^{28,54} while others excluded entire scans due to excessive motion.^{23,25,28,55,56} Here, we implemented both motion scrubbing and scan exclusions. After the preprocessing steps and applying the user-independent exclusion criteria, there were considerably more discarded scans in the awake database than in the lightly sedated group. Furthermore, the motion parameters obtained from the motion correction showed that most of the scans in the lightly sedated group had a translation of less than 1 voxel in all directions of translation and of less than 3 degrees in all directions of rotation.

The effects of light sedation have not yet been described in detail in the literature, and our openly available data provide an opportunity to study this aspect. In many studies, sedation during fMRI has been achieved with 0.5% isoflurane and a low dose of medetomidine, as it yields a state that resembles well the awake state both in mice and rats.^{23,32,57} Therefore, our data provide a unique opportunity to investigate the individual effect of isoflurane on FC in the commonly used anesthesia protocol involving a mixture of isoflurane-medetomidine. However, the effects of different anesthetics are likely not additive, which makes it difficult to draw definitive conclusions related to the overall effects of isoflurane-medetomidine sedation without conducting further experiments.

There are no studies comparing FC between the low dose of isoflurane and isoflurane-medetomidine groups. In our previous work,²³ the isoflurane-medetomidine group showed 0.1–0.2 smaller cortical correlation coefficients compared with the awake group, and the differences were even greater in subcortical regions. In another study conducted in mice,³⁷ the FC was widely decreased (up to 0.4 difference in correlation coefficients) during isoflurane-medetomidine sedation compared with the awake state. In our current work, the correlation coefficient differences between lightly sedated and awake data were less than 0.1 in the majority of edges. These observations would indicate that even although the FC under the isoflurane-medetomidine protocol resembles relatively well the awake state, the implementation of the lightly sedated protocol can bring the FC significantly closer to the awake state compared with the isoflurane-medetomidine protocol.

A limitation of our study is that we used only male rats and therefore potential sex-related differences could not be investigated. One challenge encountered here was the different number of acquired volumes in different groups. The number of volumes in the open awake database varied between 600 and 1200. On average, there were twice as many volumes in the onsite-measured data. Even if only selected windows were used in the analysis in both groups, this could lead to some bias in the comparison between the groups, as there is a certain degree of temporal

variability due to the initial isoflurane exposure. Another challenge is the vastly different number of scans in the comparison with the onsite measurements. Despite the careful choice of the statistical test, the statistical power may be limited here. It is also worth noting that dynamic properties were not explored in this work beyond assessing the lingering effect of initial anesthesia. It has been shown that anesthesia influences the dynamic FC,⁵⁷ but the effect of light anesthesia on the dynamic FC has yet to be determined. Similarly, it has been suggested that network organization is modulated by anesthesia.³⁸ These are potential topics for future studies.

In summary, the similarity of the FC obtained in awake and lightly sedated conditions indicates that light sedation after a short habituation protocol can provide a good alternative approach for large-scale fMRI studies. Even although the light sedation protocol has minor confounding effects of anesthesia on FC, the protocol can be a particularly good option if the awake fMRI approach becomes prohibitively too time-consuming. Importantly, the light sedation protocol minimizes the motion of the animal during the acquisition and increases the amount of data that can be used in the analyses. Moreover, there is considerably less stress experienced by the lightly sedated rats compared with the fully awake rats.²⁹ Thus, the short habituation time provides the greatest benefits in longitudinal studies and in experiments with a large number of animals, where it can save hundreds of training days. Nevertheless, in studies with a small number of animals, the awake protocol still provides results in which anesthesia exerts the least confounding effects.

ACKNOWLEDGMENTS

We would like to thank Professor Jussi Tohka for the advice on the statistical analysis. This project is cofunded by the Horizon 2020 Framework Programme of the European Union (Marie Skłodowska Curie grant agreement no. 740264) and the Academy of Finland (grant no. 298007).

DATA AVAILABILITY STATEMENT

The data that support the findings of this study are openly available in Fairdata at <https://doi.org/10.23729/e5d42218-b1f9-4f1c-83fa-2356cc2a6b61>.

ORCID

Lenka Dvořáková  <https://orcid.org/0000-0003-0880-4743>

Petteri Stenroos  <https://orcid.org/0000-0002-4733-5014>

Olli Gröhn  <https://orcid.org/0000-0003-1372-1651>

REFERENCES

1. Biswal B, Zerrin Yetkin F, Haughton VM, Hyde JS. Functional connectivity in the motor cortex of resting human brain using echo-planar mri. *Magn Reson Med*. 1995;34(4):537-541. doi:10.1002/mrm.1910340409
2. Xue J, Guo H, Gao Y, et al. Altered directed functional connectivity of the hippocampus in mild cognitive impairment and Alzheimer's disease: a resting-state fMRI study. *Front Aging Neurosci*. 2019;11(December):1-15. doi:10.3389/fnagi.2019.00326
3. Centeno M, Carmichael DW. Network connectivity in epilepsy: Resting state fMRI and EEG-fMRI contributions. *Front Neurol*. 2014;5(July):93. doi:10.3389/fneur.2014.00093
4. Itahashi T, Yamada T, Watanabe H, et al. Altered Network Topologies and Hub Organization in Adults with Autism: A Resting-State fMRI Study. *PLoS ONE*. 2014;9(4):e94115. doi:10.1371/journal.pone.0094115
5. Engels G, Vlaar A, McCoy B, Scherder E, Douw L. Dynamic functional connectivity and symptoms of Parkinson's disease: a resting-state fMRI study. *Front Aging Neurosci*. 2018;23(10):388. doi:10.3389/fnagi.2018.00388
6. Li M, Xu H, Lu S. Neural basis of depression related to a dominant right hemisphere: A resting-state fMRI study. *Behav Neurol*. 2018;2018:5024520. doi:10.1155/2018/5024520
7. Wang S, Zhan Y, Zhang Y, et al. Abnormal long- and short-range functional connectivity in adolescent-onset schizophrenia patients: A resting-state fMRI study. *Prog Neuropsychopharmacol Biol Psychiatry*. 2018;81:445-451. doi:10.1016/j.pnpbp.2017.08.012
8. Xu K, Liu H, Li H, et al. Amplitude of low-frequency fluctuations in bipolar disorder: A resting state fMRI study. *J Affect Disord*. 2014;152-154(1):237-242. doi:10.1016/j.jad.2013.09.017
9. Faragó P, Tuka B, Tóth E, et al. Interictal brain activity differs in migraine with and without aura: resting state fMRI study. *J Headache Pain*. 2017;18(1): 8. doi:10.1186/s10194-016-0716-8
10. Amin FM, Hougaard A, Magon S, et al. Altered thalamic connectivity during spontaneous attacks of migraine without aura: A resting-state fMRI study. *Cephalalgia*. 2018;38(7):1237-1244. doi:10.1177/0333102417729113
11. Coppola G, di Renzo A, Petolicchio B, et al. Aberrant interactions of cortical networks in chronic migraine: A resting-state fMRI study. *Neurology*. 2019;92(22):E2550-E2558. doi:10.1212/WNL.00000000000007577
12. Zhang J, Su J, Wang M, et al. The sensorimotor network dysfunction in migraineurs without aura: a resting-state fMRI study. *J Neurol*. 2017;264(4): 654-663. doi:10.1007/s00415-017-8404-4
13. Hori Y, Schaeffer DJ, Yoshida A, et al. Cortico-subcortical functional connectivity profiles of resting-state networks in marmosets and humans. *J Neurosci*. 2020;40(48):9236-9249. doi:10.1523/JNEUROSCI.1984-20.2020
14. Gao YR, Ma Y, Zhang Q, et al. Time to wake up: Studying neurovascular coupling and brain-wide circuit function in the un-anesthetized animal. *Neuroimage*. 2017;153:382-398. doi:10.1016/J.NEUROIMAGE.2016.11.069
15. Lu H, Zou Q, Gu H, Raichle ME, Stein EA, Yang Y. Rat brains also have a default mode network. *Proc Natl Acad Sci U S A*. 2012;109(10):3979-3984. doi:10.1073/pnas.1200506109

16. Becerra L, Pendse G, Chang PC, Bishop J, Borsook D. Robust reproducible resting state networks in the awake rodent brain. *PLoS ONE*. 2011;6(10):e25701. doi:[10.1371/journal.pone.0025701](https://doi.org/10.1371/journal.pone.0025701)
17. Paasonen J, Laakso H, Pirttimäki T, et al. Multi-band SWIFT enables quiet and artefact-free EEG-fMRI and awake fMRI studies in rat. *Neuroimage*. 2020;206:116338. doi:[10.1016/j.neuroimage.2019.116338](https://doi.org/10.1016/j.neuroimage.2019.116338)
18. Jonckers E, Delgado y Palacios R, Shah D, Guglielmetti C, Verhoye M, van der Linden A. Different anesthesia regimes modulate the functional connectivity outcome in mice. *Magn Reson Med*. 2014;72(4):1103-1112. doi:[10.1002/mrm.24990](https://doi.org/10.1002/mrm.24990)
19. Liang Z, Watson GDR, Alloway KD, Lee G, Neuberger T, Zhang N. Mapping the functional network of medial prefrontal cortex by combining optogenetics and fMRI in awake rats. *Neuroimage*. 2015;117:114-123. doi:[10.1016/j.neuroimage.2015.05.036](https://doi.org/10.1016/j.neuroimage.2015.05.036)
20. Christie IN, Wells JA, Southern P, et al. fMRI response to blue light delivery in the naïve brain: Implications for combined optogenetic fMRI studies. *Neuroimage*. 2013;66:634-641. doi:[10.1016/j.neuroimage.2012.10.074](https://doi.org/10.1016/j.neuroimage.2012.10.074)
21. Wehrl HF, Hossain M, Lankes K, et al. Simultaneous PET-MRI reveals brain function in activated and resting state on metabolic, hemodynamic and multiple temporal scales. *Nat Med*. 2013;19(9):1184-1189. doi:[10.1038/nm.3290](https://doi.org/10.1038/nm.3290)
22. Schulz K, Sydekum E, Krueppel R, et al. Simultaneous BOLD fMRI and fiber-optic calcium recording in rat neocortex. *Nat Methods*. 2012;9(6):597-602. doi:[10.1038/nmeth.2013](https://doi.org/10.1038/nmeth.2013)
23. Paasonen J, Stenroos P, Salo RA, Kiviniemi V, Gröhn O. Functional connectivity under six anesthesia protocols and the awake condition in rat brain. *Neuroimage*. 2018;172:9-20. doi:[10.1016/j.neuroimage.2018.01.014](https://doi.org/10.1016/j.neuroimage.2018.01.014)
24. Chen X, Tong C, Han Z, et al. Sensory evoked fMRI paradigms in awake mice. *Neuroimage*. 2020;204:116242. doi:[10.1016/j.neuroimage.2019.116242](https://doi.org/10.1016/j.neuroimage.2019.116242)
25. Harris AP, Lennen RJ, Marshall I, et al. Imaging learned fear circuitry in awake mice using fMRI. *Eur J Neurosci*. 2015;42(5):2125-2134. doi:[10.1111/ejn.12939](https://doi.org/10.1111/ejn.12939)
26. Cai X, Qiao J, Kulkarni P, Harding IC, Ebong E, Ferris CF. Imaging the effect of the circadian light-dark cycle on the glymphatic system in awake rats. *Proc Natl Acad Sci U S A*. 2020;117(1):668-676. doi:[10.1073/pnas.1914017117](https://doi.org/10.1073/pnas.1914017117)
27. King JA, Garelick TS, Brevard ME, et al. Procedure for minimizing stress for fMRI studies in conscious rats. *J Neurosci Methods*. 2005;148(2):154-160. doi:[10.1016/j.jneumeth.2005.04.011](https://doi.org/10.1016/j.jneumeth.2005.04.011)
28. Liu Y, Perez PD, Ma Z, et al. An open database of resting-state fMRI in awake rats. *Neuroimage*. 2020;220:117094. doi:[10.1016/j.neuroimage.2020.117094](https://doi.org/10.1016/j.neuroimage.2020.117094)
29. Stenroos P, Paasonen J, Salo RA, et al. Awake rat brain functional magnetic resonance imaging using standard radio frequency coils and a 3D printed restraint kit. *Front Neurosci*. 2018;12(AUG):548. doi:[10.3389/fnins.2018.00548](https://doi.org/10.3389/fnins.2018.00548)
30. Avants BB, Tustison N, Song G. Advanced normalization tools (ANTS). *Insight J*. 2009;2(365):1-35. www.picsl.upenn.edu/ANTS. Accessed July 15, 2021
31. Paxinos G, Watson C. *The Rat Brain in Stereotaxic Coordinates*. 4th ed.
32. Grandjean J, Canella C, Anckaerts C, et al. Common functional networks in the mouse brain revealed by multi-centre resting-state fMRI analysis. *Neuroimage*. 2020;205:116278. doi:[10.1016/J.NEUROIMAGE.2019.116278](https://doi.org/10.1016/J.NEUROIMAGE.2019.116278)
33. Barrière DA, Magalhães R, Novais A, et al. The SIGMA rat brain templates and atlases for multimodal MRI data analysis and visualization. *Nat Commun*. 2019;10(1):5699. doi:[10.1038/s41467-019-13575-7](https://doi.org/10.1038/s41467-019-13575-7)
34. Avants BB, Epstein CL, Grossman M, Gee JC. Symmetric diffeomorphic image registration with cross-correlation: evaluating automated labeling of elderly and neurodegenerative brain. *Med Image Anal*. 2008;12(1):26-41. doi:[10.1016/j.media.2007.06.004](https://doi.org/10.1016/j.media.2007.06.004)
35. Chung E, Romano JP. Exact and asymptotically robust permutation tests. *Annal Stat*. 2013;41(2):484-507. doi:[10.1214/13-AOS1090](https://doi.org/10.1214/13-AOS1090)
36. Benjamini Y, Hochberg Y. Controlling the false discovery rate: a practical and powerful approach to multiple testing. *J R Stat Soc B Methodol*. 1995; 57(1):289-300. doi:[10.1111/J.2517-6161.1995.TB02031.X](https://doi.org/10.1111/J.2517-6161.1995.TB02031.X)
37. Tsurugizawa T, Yoshimaru D. Impact of anesthesia on static and dynamic functional connectivity in mice. *Neuroimage*. 2021;241:118413. doi:[10.1016/J.NEUROIMAGE.2021.118413](https://doi.org/10.1016/J.NEUROIMAGE.2021.118413)
38. Liang Z, King J, Zhang N. Intrinsic organization of the anesthetized brain. *J Neurosci*. 2012;32(30):10183-10191. doi:[10.1523/JNEUROSCI.1020-12.2012](https://doi.org/10.1523/JNEUROSCI.1020-12.2012)
39. Fox MD, Zhang D, Snyder AZ, Raichle ME. The global signal and observed anticorrelated resting state brain networks. *J Neurophysiol*. 2009;101(6): 3270-3283. doi:[10.1152/JN.90777.2008](https://doi.org/10.1152/JN.90777.2008)
40. Aquino KM, Fulcher BD, Parkes L, Sabaroeidin K, Fornito A. Identifying and removing widespread signal deflections from fMRI data: Rethinking the global signal regression problem. *Neuroimage*. 2020;212:116614. doi:[10.1016/J.NEUROIMAGE.2020.116614](https://doi.org/10.1016/J.NEUROIMAGE.2020.116614)
41. Liu X, Zhu XH, Zhang Y, Chen W. The change of functional connectivity specificity in rats under various anesthesia levels and its neural origin. *Brain Topogr*. 2013;26(3):363-377. doi:[10.1007/S10548-012-0267-5](https://doi.org/10.1007/S10548-012-0267-5)
42. Liu TT, Nalci A, Falahpour M. The global signal in fMRI: Nuisance or information? *Neuroimage*. 2017;150:213-229. doi:[10.1016/J.NEUROIMAGE.2017.02.036](https://doi.org/10.1016/J.NEUROIMAGE.2017.02.036)
43. Power JD, Plitt M, Laumann TO, Martin A. Sources and implications of whole-brain fMRI signals in humans. *Neuroimage*. 2017;146:609-625. doi:[10.1016/J.NEUROIMAGE.2016.09.038](https://doi.org/10.1016/J.NEUROIMAGE.2016.09.038)
44. Saad ZS, Gotts SJ, Murphy K, et al. Trouble at rest: how correlation patterns and group differences become distorted after global signal regression. *Brain Connect*. 2012;2(1):25-32. doi:[10.1089/BRAIN.2012.0080](https://doi.org/10.1089/BRAIN.2012.0080)
45. Aggarwal A, Brennan C, Shortal B, Contreras D, Kelz MB, Proekt A. Coherence of visual-evoked gamma oscillations is disrupted by propofol but preserved under equipotent doses of isoflurane. *Front Syst Neurosci*. 2019;13:19. doi:[10.3389/fnsys.2019.00019](https://doi.org/10.3389/fnsys.2019.00019)
46. Guidera JA, Taylor NE, Lee JT, et al. Sevoflurane induces coherent slow-delta oscillations in rats. *Front Neural Circuits*. 2017;11:36. doi:[10.3389/fncir.2017.00036](https://doi.org/10.3389/fncir.2017.00036)
47. Liu X, Zhu XH, Zhang Y, Chen W. Neural origin of spontaneous hemodynamic fluctuations in rats under burst-suppression anesthesia condition. *Cereb Cortex*. 2011;21(2):374-384. doi:[10.1093/cercor/bhq105](https://doi.org/10.1093/cercor/bhq105)
48. Zhao W, Zhao S, Zhu T, et al. Isoflurane suppresses hippocampal high-frequency ripples by differentially modulating pyramidal neurons and interneurons in mice. *Anesthesiology*. 2021;135(1):122-135. doi:[10.1097/ALN.0000000000003803](https://doi.org/10.1097/ALN.0000000000003803)

49. Stenroos P, Pirttimäki T, Paasonen J, et al. Isoflurane affects brain functional connectivity in rats 1 month after exposure. *Neuroimage*. 2021;234:117987. doi:[10.1016/J.NEUROIMAGE.2021.117987](https://doi.org/10.1016/J.NEUROIMAGE.2021.117987)
50. Thrane AS, Thrane VR, Zeppenfeld D, et al. General anesthesia selectively disrupts astrocyte calcium signaling in the awake mouse cortex. *Proc Natl Acad Sci U S A*. 2012;109(46):18974-18979. doi:[10.1073/PNAS.1209448109](https://doi.org/10.1073/PNAS.1209448109)
51. Bukhari Q, Schroeter A, Cole DM, Rudin M. Resting state fMRI in mice reveals anesthesia specific signatures of brain functional networks and their interactions. *Front Neural Circuits*. 2017;11:5. doi:[10.3389/FNCIR.2017.00005/BIBTEX](https://doi.org/10.3389/FNCIR.2017.00005/BIBTEX)
52. Power JD, Mitra A, Laumann TO, Snyder AZ, Schlaggar BL, Petersen SE. Methods to detect, characterize, and remove motion artifact in resting state fMRI. *Neuroimage*. 2014;84:320-341. doi:[10.1016/J.NEUROIMAGE.2013.08.048](https://doi.org/10.1016/J.NEUROIMAGE.2013.08.048)
53. Masaki Y, Kashiwagi Y, Watabe H, Abe K. (R)- and (S)-ketamine induce differential fMRI responses in conscious rats. *Synapse*. 2019;73(12):e22126. doi:[10.1002/SYN.22126](https://doi.org/10.1002/SYN.22126)
54. Ma Z, Perez P, Ma Z, et al. Functional atlas of the awake rat brain: A neuroimaging study of rat brain specialization and integration. *Neuroimage*. 2018;170:95-112. doi:[10.1016/j.neuroimage.2016.07.007](https://doi.org/10.1016/j.neuroimage.2016.07.007)
55. Harris AP, Lennen RJ, Brydges NM, et al. The role of brain-derived neurotrophic factor in learned fear processing: an awake rat fMRI study. *Genes Brain Behav*. 2016;15:221-230. doi:[10.1111/gbb.12277](https://doi.org/10.1111/gbb.12277)
56. Liang Z, King J, Zhang N. Neuroplasticity to a single-episode traumatic stress revealed by resting-state fMRI in awake rats. *Neuroimage*. 2014;103:485-491. doi:[10.1016/j.neuroimage.2014.08.050](https://doi.org/10.1016/j.neuroimage.2014.08.050)
57. Liang Z, Liu X, Zhang N. Dynamic resting state functional connectivity in awake and anesthetized rodents. *Neuroimage*. 2015;104:89-99. doi:[10.1016/j.neuroimage.2014.10.013](https://doi.org/10.1016/j.neuroimage.2014.10.013)

SUPPORTING INFORMATION

Additional supporting information may be found in the online version of the article at the publisher's website.

How to cite this article: Dvořáková L, Stenroos P, Paasonen E, Salo RA, Paasonen J, Gröhn O. Light sedation with short habituation time for large-scale functional magnetic resonance imaging studies in rats. *NMR in Biomedicine*. 2022;35(6):e4679. doi:[10.1002/nbm.4679](https://doi.org/10.1002/nbm.4679)